Seafloor compliance: Project Number C46-19-1

Report 5: Interpretation and Summary

Wayne C. Crawford and Satish C. Singh

Project Introduction

This project was funded by the SINDRI consortium for a total of 1,384,396 Danish Kroner. The funding supported a one-year postdoctoral position, 3.5 days of ship time on the Faroese Fisheries vessel Magnus Heinasson, rental and insurance of two seafloor compliance sensors and transportation and travel. The project was proposed in 1 February 2002, in response to the SINDRI phase 1 call for proposals, and a contract was signed in September 2003. The original schedule was for 2 seafloor compliance measurements in summer 2004 and final interpretation by October 2005.

This schedule was modified twice: once to push the cruise back to winter 2004 for scientific reasons explained below and once to allow time to find a new postdoctoral researcher after our first postdoc obtained a permanent position elsewhere.

The project timeline was:

Item	Date	Comments
Initial Proposal submitted	1 February 2002	
Detailed Proposal submitted	29 March 2002	
Contract signed		
Site Selection and Sensitivity Report	January 2004	Deliverable #1:
Site Selection update	July 2004	
Data collection Cruise	Nov-Dec 2004	
Data and data acquisition Report	1 February 2005	Deliverable #2: originally scheduled 1 August 2004
Data Processing Report	1 June 2005	Deliverable #3: originally scheduled 1 January 2005
Data Integration Report	28 January 2006	Deliverable #4: originally scheduled 1 April 2005
Interpretation (Final) Report	June 2006	Deliverable #5: originally scheduled 1 October 2005

Scientific Introduction

We measured seafloor accelerations and pressure at three sites in the Faeroes-Shetland basin. Our goal was to determine the sensitivity of seafloor compliance measurements to sub-basalt sediments in this basin. Seafloor compliance — the seafloor motion under pressure forcing from ocean surface waves — is sensitive to subsurface shear moduli, and particularly to low shear modulus zones associated with trapped fluids [*Crawford et al.*, 1991]. A theoretical case study [*Crawford*, 2004] indicated that compliance measurements should be sensitive to sub-basalt sediments, but various parameters particular to the Faeroes-Shetland basin were unknown. In particular, the strength of the forcing pressure waves and the shear modulus of the sub-basalt sediments strongly affect how well compliance can be measured, and were until now unknown.

We obtained SINDRI funding to measure the components of seafloor compliance in the Faeroes-Shetland basin. The SINDRI consortium funded us for two measurements, and we financed 4 more days of ship time so that we could attempt six measurements. We added these attempts mostly by prudence: seafloor compliance sensors are delicate and the instruments that we were to use were recently constructed. In addition, obtaining more than two measurements would allow us to better explore variations in subsurface structure and the forcing infragravity wave signal. We placed our sites on pre-existing seismic and electromagnetic measurement lines to allow us to compare the information obtainable by the different methods, and we choose generally deep sites where compliance measurements would be sensitive to the deepest structure.

Of our six measurements, three gave useful pressure and acceleration data. The data has a high noise level, probably due to strong bottom currents. There is also a strong variation in the ocean surface wave pressure signal between sites, with the signal much stronger in the middle of the basin than on the Faeroes plateau. We were able to calculate compliance at two of the sites, at relatively high frequencies that only penetrate to two km beneath the seafloor. Our data therefore do not constrain the sub-basalt sediments. The sediments above the basalt flows, however, are well constrained. The site on the Faeroe plateau has much lower shear modulus than the site in Faeroe basin.

We present the experiment, data, inversions and interpretation herein. At the end, we discuss the feasibility of compliance measurements for sub-basalt measurements in light of the data collected.

Site description

The Faeroe Basin, located between the Shetland and Faeroe Islands, is an extensional system belonging to the northwestern European passive margin. It results from the continental break up and subsequent opening of the North Atlantic in the early Tertiary. The presence of the Iceland mantle plume beneath the margin at the time of break up resulted in an enhanced melt production [*White and McKenzie*, 1989] and important basalt floods. Due to the thermal subsidence of the margin following its formation, the basalt flowed southeastward from its area of extrusion, west of the present Faeroe Islands, to the centre of the basin, some 150 km away, overlying Mesozoic to Early Tertiary sedimentary units in the process. A basaltic layer, whose thickness decreases from about 5 km in the Faeroe Islands [*Richardson et al.*, 1998] to zero on its southeastern fringe, was thus emplaced on a large surface of the Faeroe Basin. Subsequent subsidence and sedimentation have resulted in the presently observed structures which are, from top to bottom, 1 to 2 km of Tertiary sediments, a basaltic layer of 0 to 3 km thickness in the northwestern part of

the basin, Mesozoic to early Palaeocene sediments (up to 8 km thick at the centre of the basin) and finally, an igneous continental basement, probably of Lewisian age and possibly intruded by Tertiary basaltic sills. The basaltic layer is itself divided into units separated by thin interbedded sedimentary deposits [*White et al.*, 2003].

The uppermost subbasaltic sediments were deposited in a context of active extensional tectonics, which resulted in the emplacement of hydrocarbon bearing fans that are well identified through classical multichannel seismic imaging in the basalt-free locations of the basin. It is quite likely that such features also exist underneath the basalt.

Problem

It is difficult to image sediments beneath basalt flows. Traditional seismic reflection methods are thwarted by the large number of reflectors within the basalts [*White et al.*, 1999; *Martini and Bean*, 2001; *Ziolkowski et al.*, 2002]. Wide-angle seismic imaging is more promising and both wide-angle OBS experiments [*Hughes et al.*, 1997; *Hughes et al.*, 1998] and 2-ship experiments have penetrated beneath the basalt flows [*White et al.*, 1999; *Fliedner and White*, 2003; *Jones*, 2003; *White et al.*, 2003]. Low frequency seismic sources can also penetrate the basalt flows, at the cost of lower resolution. Seismic techniques constrain mostly P wave properties, because immersed marine seismic sources only generate P waves. Marine electromagnetic measurements have also recently been tested with SINDRI funding as a way to determine the fluid content and connectivity of sub-basalt sediments by constraining their resistivity (Jegen, 2005).

A good knowledge of the shear properties of the medium is fundamental to assess the presence of fluids such as hydrocarbons. Marine seismic experiments can excite subsurface S waves by the conversion of incident P waves which can then be measured directly at the seafloor by OBSs [*Fruehn et al.*] or as reconverted P arrivals by seismic streamers [*Fliedner and White*, 2003]. In either case, one has to rely on mode conversions, which make it difficult to identify and exploit S waves.

Seafloor compliance is a relatively new geophysical prospecting technique that is primarily sensitive to the subsurface shear modulus [*Yamamoto and Torii*, 1986; *Yamamoto et al.*, 1989; *Crawford et al.*, 1991; *Crawford et al.*, 1998; *Latychev and Edwards*, 2003]. In addition, compliance is particularly sensitive to low shear modulus zones associated with fluids and is largely insensitive to seismic reflectors. Compliance is the seafloor deformation under ocean waves as a function of frequency. Since these waves are much slower than S and P wave velocities in the subsurface, little or no seismic waves are excited and a compliance measurement is sensitive to structure directly beneath the measurement site. Compliance has relatively low vertical resolution but can be sensitive to very thin low velocity zones. Compliance measurements and seismic measurements complement one another: The sensitivity of compliance measurements to the subsurface shear modulus complements the sensitivity of active seismic experiments to P wave velocities and acoustic impedance contrasts, and the high resolution of seismic reflection can improve the vertical resolution of shear modulus models obtained from compliance measurements. Compliance is measured by deploying a broadband seismometer and differential pressure gauge to the seafloor for two or more days. The depth sensitivity of compliance is proportional to the forcing wavelength, and compliance measurements across a range of frequencies (typically 0.003 to 0.1 Hz) are sensitive to structure over a range of depths. Multiple compliance measurements can be used to create 2-D or 3-D subsurface shear modulus models.

Compliance measurements rely on a natural source: long-period (10-1000 seconds) ocean surface gravity waves known as *infragravity* waves [*Webb et al.*, 1991]. These waves are very small (1-10 mm tall) and very long (from ocean depth to several tens of km) and thus are effectively invisible at the sea surface.

They are detectable at the seafloor thanks to their long wavelength, which allows their pressure signal to reach the seafloor unattenuated whereas much larger wind waves with wavelengths shorter than the ocean depth contribute no detectable seafloor signal.

Infragravity waves are thought to be generated by non-linear wave-wave interactions under storms in shallow water [*Snodgrass et al.*, 1966; *Gallagher*, 1971; *Guza and Bowen*, 1976; *Okihiro et al.*, 1992; *Herbers et al.*, 1994; *Herbers et al.*, 1995a; *Herbers et al.*, 1995b]. Because infragravity waves are generally several km long, most of their energy is trapped at coastlines, but some energy leaks out and can traverse oceans unattenuated. The exact processes creating infragravity waves and allowing them to escape coastlines are only vaguely understood and difficult to model and the only way to reliably determine the infragravity wave signal at a given location is to directly measure it at the seafloor. Before the present experiment, this had only been done in the Pacific Ocean, at one site in the North Atlantic Ocean and at one site in the Arctic Ocean [*Webb et al.*, 1991; *Webb*, 1998]. The Pacific Ocean signal is relatively steady in time and space, with a strength of about 10^5 Pa^2/Hz. The Atlantic Ocean signal was, however, much smaller (**Figure 1**) and varied with time. Webb [*Webb et al.*] explained this by the small amount of stormy coastline within direct wave path of the Atlantic site, which is blocked from latitudes above 40°N by the Labrador shelf and which sees very little coastline below the equator because of blocking by the African and South American continents.

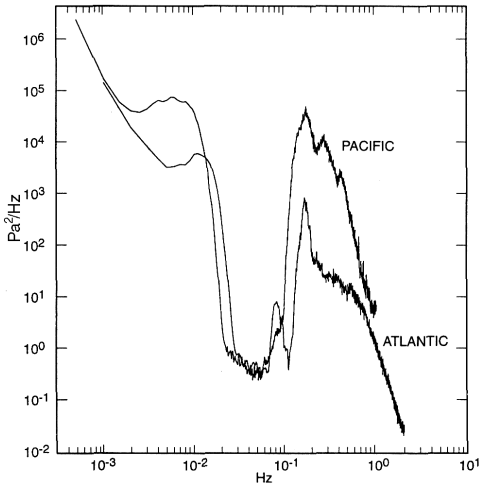

Figure 1: Difference in infragravity wave signals (signals below 0.1 Hz) between Pacific Ocean and Atlantic Ocean sites (from [*Webb et al.*, 1991]5]5]).

Compliance is sensitive to structure at approximately 1/5 the wavelength of the forcing ocean waves. These wavelengths are governed by the linear ocean surface gravity wave dispersion equation:

$$\omega^2 = gk\tanh(kH) \qquad (1)$$

where ω is the angular frequency, g is the gravitational acceleration, k is the wavenumber, H is the water depth and the wavelength, $\lambda \equiv 2\pi / k$. The highest frequency at which compliance can be measured corresponds approximately to $\lambda = H$ and the lowest frequency, controlled by the seismological noise level, is approximately 0.003 Hz. Therefore, compliance measurements should be sensitive to structure at subsurface depths between 50 and 4000 m at 500 m water depth and between 200 and 7000 m at 1500 m water depth [*Crawford*, 2004].

Modelling indicates that compliance measurements should be sensitive to sub-basalt sediments if the pressure signal is greater than 10^4 Pa^2/Hz [*Crawford*, 2004], but we did not know if the Faeroes basin had pressure signals this high. In theory, it should have a higher infragravity wave signal level than the Atlantic Ocean site because it is within the ocean wave path of much more stormy, high latitude coastline, but this remained to be proved by measurements. The bathymetric effect also needed to be studied: with the most promising sites for hydrocarbon exploration located in the deepest waters, would most of the infragravity wave energy be bathymetrically steered away from these areas into shallower waters?

Approach

We decided to measure seafloor pressure and acceleration (from which compliance can be calculated) at as many sites as possible, to allow us to see variations in subsurface structure, but also to investigate

possible spatial variations in the infragravity wave signal and as an insurance policy against instrument problems. The compliance signal is much smaller and longer period than that measured by conventional OBSs and so we use custom OBSs containing relatively delicate and complicated broadband seismometers. As the previous generation of compliance instruments were too large and cumbersome to be opened in case of problems on a small ship, we used recently developed modular sensors that could be opened on a small ship. We could also rapidly download data from these instruments between deployments within opening them, allowing us to rapidly backup the data and prepare the instruments for redeployment. We had two instruments for the experiment, so six measurements required redeploying each one twice.

We chose to deploy our instruments along pre-existing seismic lines, mostly in the deep waters where compliance would be most sensitive to sub-basalt structure and where the thinner basalt layer would make exploration drilling easier. We choose the FLARE seismic lines 1 and 10. FLARE 1 has been well processed and appears to have excited the most industry interest. FLARE 10 was interested because electromagnetic data were recently collected along it, and it crosses the recently acquired iSIMM line [*White et al.*, 2002] near the basin axis. We were funded by SINDRI for two measurements and we added our own funding to obtain four more deployments. Two deployments would be on the FLARE 10 line within the Faeroes basin and four deployments would be on the FLARE 10 line, going from the middle of the basin to the edge of the Faeroes plateau (**Figure 2**). To maximize our chances of finding strong infragravity wave energy, we decided to deploy at the end of the ship's season, at the very end of November 2004.

Data collection

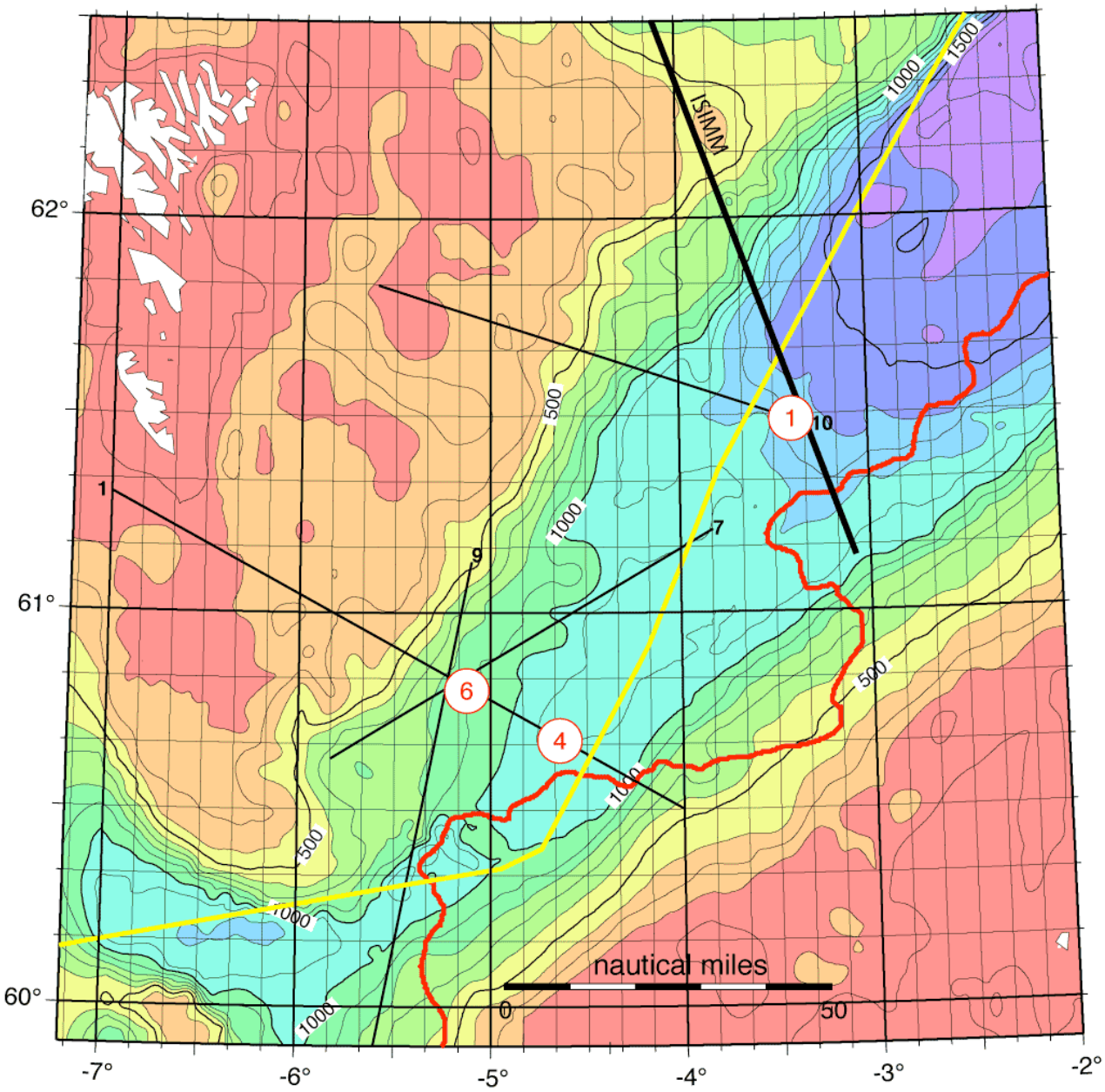

Figure 2: Compliance measurement sites. Seismic lines from the FLARE and iSIMM experiments passing over or near the compliance sites are shown, as is the boundary of the Faeroes basalt flows (red line) and Faeroes waters (yellow line).

The compliance sensors were shipped from New York to our laboratories in Paris, France a couple of months before the cruise, so that we could train on them. They were subsequently shipped to Thorshavn, Faeroes a couple of weeks before the cruise. We deployed the compliance sensors using the Faeroes Fishery vessel Magnus Heinasson. The details of this cruise are outlined in the cruise report, delivered with report 2: "Cruise and Initial Data Analysis". Deployments and recoveries had to be done in two stages because there was no access to the water from the level where we stored and worked on the

compliance sensors. Deployments had to be made from a rather high level, which added to the pendulum arm of the compliance sensor as it was being lowered into the ocean. One instrument was plagued by bad luck: on at least one occasion it swung into the side of the ship while being lowered into the sea. On a subsequent deployment, the seismometer's levelling system came loose and the instrument could not level at the seafloor. We repaired the levelling system at sea and opened the other instrument to confirm that its levelling system was ok. Finally, the data from the unlucky instrument, while visually acceptable, did not give acceptable spectra. We were not able to confirm these spectra onboard the ship because the instruments were delivered to us uncalibrated (very few groups in the world calibrate their differential pressure gauges). After we calibrated the instruments post-cruise, we discovered that instrument 1 had a problem.

A post-cruise autopsy on instrument 1 revealed that one of the negative analogue power batteries went to zero volts under a load of 1 kiloOhm or less. The countdown before each deployment includes a software voltage test under load for digital power and positive analogue power, but not for negative analogue power. The data from sites 2, 3 and 5 are therefore useless.

Data analysis

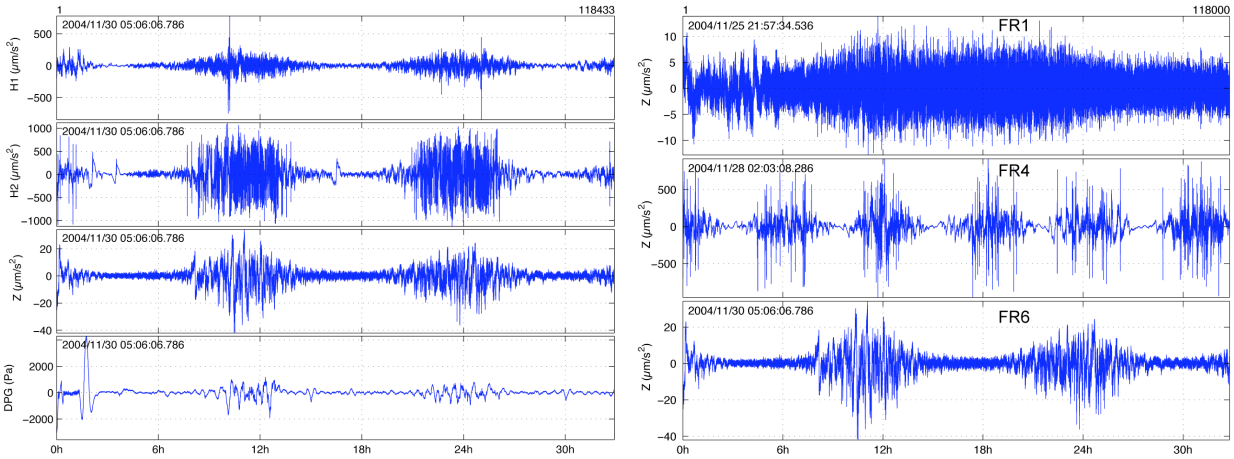

Figure 3: Seafloor data time series. Left: All channels, site FR6. Right: Vertical channel, all sites.

We recalibrated both the seismometers and differential pressure gauges post-cruise to confirm the instrument responses we had been provided pre-cruise (report #3: Data Processing). The seismometer instrument response was the same as we had been told, but the differential pressure gauges had apparently not been carefully calibrated before. This didn't surprise us, as most laboratories do not calibrate their differential pressure gauges.

We next plotted data time series for each channel, corrected for the instrument response (**Figure 3**). At each site and on each channel, there was a high, periodic noise with maxima 6 or 12 hours apart. The noise spectra are consistent with seafloor currents [*Crawford and Webb*, 2000], while the noise period corresponds well with tidal current maxima. We attribute most of this noise to extremely strong seafloor tidal currents, for which the Faeroes-Shetland basin is known [*Bonnin et al.*, 2002; *Masson et al.*, 2004]. The seismometer noise may be exacerbated by a grounding problem that could have fed-back noise into the system. Our colleagues at the Lamont-Doherty Earth Observatory are still investigating this possibility

The noise levels are different at each site: the noise is 70 times stronger at FR4 than at FR1. To detect compliance at all the noise level must be below 1 μm/s^2/sqrt(Hz) on the vertical channel between 0.001 and 0.1 Hz and to constrain sub-basalt sediments it must be below 0.01 μm/s^2/sqrt(Hz) (we usually obtain noise levels between 0.001 and 0.01 μm/s^2/sqrt(Hz)). One can often reduce the vertical channel noise by subtracting coherent noise recorded on the horizontal channels, but the horizontal channel noise was high enough that the seismometer masses often recentered automatically, ruining their correlation with the vertical channel. We could therefore only correct the data in time windows where the noise was at its lowest.

To calculate compliance, we need to select the time windows giving the lowest uncertainty according to the formula:

$$\varepsilon(f) = \frac{\left[1-\gamma_{xy}^2(f)\right]^{1/2}}{\left|\gamma_{xy}(f)\right|\sqrt{2n_d}} \qquad (2)$$

where n is the number of data windows and $\gamma_{pa}^2(f)$ is the pressure-acceleration coherence [*Bendat and Piersol*, 1986]. We therefore require the largest possible number of data windows giving the highest pressure-acceleration coherence. We used a Monte Carlo method to select this combination (report #3: Data Processing). We use the same data windows to calculate the site spectra shown in **Figure 4**.

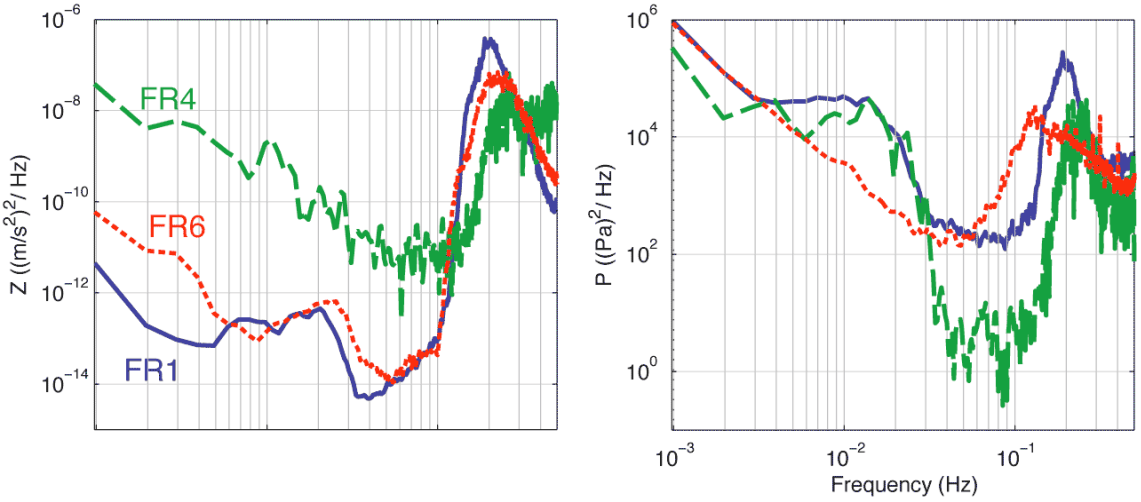

Figure 4: Signal levels at sites FR1, FR4 and FR6. Left: Vertical acceleration (compliance peak between 0.005 and 0.03 Hz). Right: pressure (infragravity waves at <0.04 Hz).

The spectra reveal that vertical channel noise is too high to see the compliance peak at site FR4 and that the infragravity wave pressure signal is much lower at site FR6 than at FR1 or FR4 (**Figure 4**). . The infragravity wave signal at sites FR1 and FR4 is $10^{4.5}$ Pa^2/Hz, strong enough to constrain sub-basalt sediments under normal noise conditions [*Crawford*, 2004]. The infragravity wave signal at site FR6 is $10^{3.5}$ Pa^2/Hz, which should be strong enough to constrain sub-basalt sediments if the noise were not so high. But the pressure and acceleration noise levels are much higher than what we have measured elsewhere, and than what Crawford [2004] assumed in modelling compliance sensitivity to subbasalt sediments. The minimum vertical seismometer noise floor of 10^-14 (m/s^2)^2/Hz is above the minimum noise level necessary to image sub-basalt sediments beneath basalts for the given infragravity wave level and crustal model of Crawford [2004]. The noise is especially damaging at the lowest frequencies, cutting off measurable compliance at 0.009 Hz rather than the usual 0.003 Hz.

We calculated compliance at sites FR1 and FR6 (**Figure 5**). Because of the high noise levels compared to the pressure signal, we developed an algorithm to separate signal and noise levels on the pressure and acceleration components, in order to calculate the compliance with the smallest possible uncertainty (report 4: data integration). The compliance is very different at the two sites.

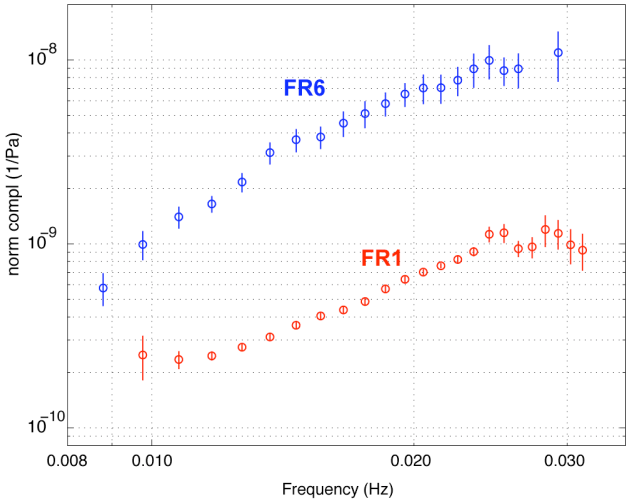

Figure 5: Faeroes Compliances.

Site FR1 is at 1380 water depth, near the eastern end of the FLARE 10 seismic line and just west of the ISIMM seismic line. It lies in the deepest part of Faeroes basin, about 5 nautical miles east of the Faeroes-UK boundary and 10 nautical miles west of the eastern limit of the Faeroes basalt flows (as determined by [*White et al.*, 2003]).

Site FR6 is at 890 meters water depth, near to the intersection of the FLARE 1, 7 and 9 seismic lines. It lies on the western side of Faeroes basin, near where the basin is most pinched.

Inversions

Depth sensitivity

After correcting for tilt noise on the vertical channel (see Data Analysis report), the compliance data spans 0.009-0.029 Hz at site FR6 and 0.01 to 0.031 Hz at site FR1. Using the average compliance depth sensitivity of 1/5 the infragravity wave wavelength at a given frequency and water depth, the data at site FR6 should be sensitive to structure at depths between 400 and 2000 m beneath the seafloor (mbsf), while site FR1 compliance should be sensitive to structure between 320 and 2100 mbsf. These maximum depths penetrate into but not beneath the basalt layer (estimated by [*White et al.*, 2003]) at site FR6 and may or may not penetrate into the basalts at site FR1. The compliances are, however, very different at the two sites, with a much higher compliance at site FR6 indicating lower shear modulus.

We ran inversions for several different model depths and model constraints to determine the shear velocity structure beneath the site (the shear modulus is constrained, but we find that most users prefer to know the corresponding shear velocity: as this depends on the assumed density, we will also provide the shear moduli in our final report).

Inversion runs

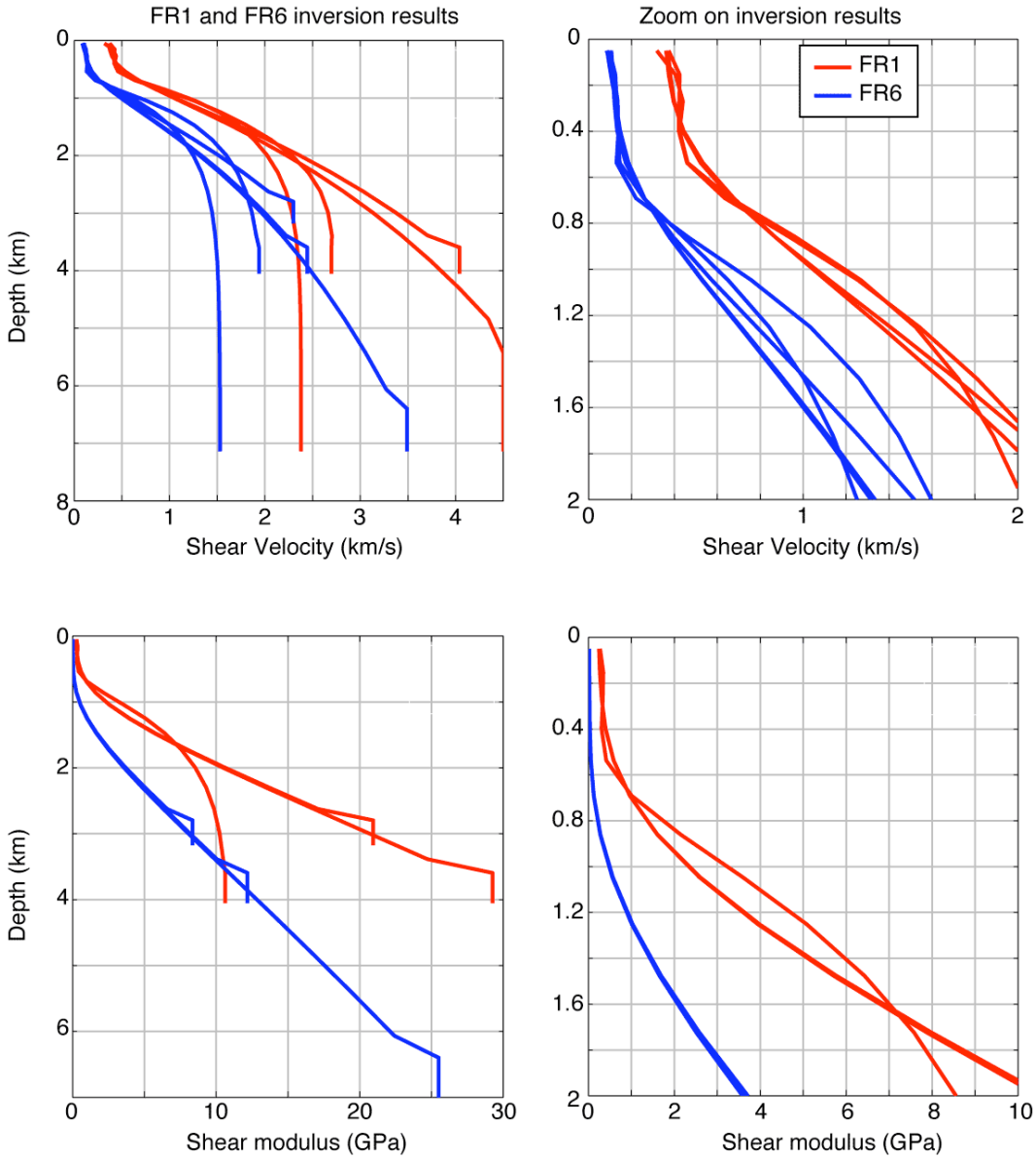

Figure 6: Inversion results for sites FR1 and FR6. Each site was inverted for models with minimum L1 and L2 norm, and maximum depths of 3000, 4000 and 7000 m. Top: Shear velocity inversions. Bottom: Shear modulus inversions.

We ran 1D inversions on the compliance data, comparing 2 different minimization functions (L1 and L2 norm) and 3 different model depth ranges (3000, 4000, and 7000 m) to determine which parts of the model were well constrained (**Figure 6**). A 2000 m model depth could not fit the data, probably because the model has to attain a certain "background" velocity much higher than that in the first 2000 meters to fit the average compliance amplitude [*Crawford et al.*, 1998]. By running several different inversions we obtain an idea of where the model is well constrained without resorting to statistical methods that depend on the compliance function being approximately linear around the solution, which it is not [*Crawford et al.*, 1991].

As predicted by our depth sensitivity estimates, the crustal structure is well constrained above approximately 2000 mbsf. At both sites, a 500-m thick low velocity top layer overlies a region of increasing shear velocity with depth. The shear velocity in the top layer is approximately 0.15 km/s at FR6 and 0.4 km/s at FR1. The velocity appears nearly constant in this layer, but this could be a depth sensitivity effect, since compliance is not sensitive to structure above about 0.3-0.4 km and the L1 minimization constraint would tend to create constant velocities in this layer. The L2 minimization constraint merely would try to keep the slope constant with that beneath the insensitive zone, so the constant velocities from about 0.3-0.5 kmbsf appear to be well constrained, as they require an L2-costly change in slope at about 0.8 kmbsf.

The FR6 velocities also appear to increase more slowly with depth than the FR1 velocities, being about 0.45 km/s slower than FR1 at 0.8 km depth and 0.7 km/s slower at 1.8 km depth. There is more uncertainty to these velocities, as can be seen by the wider spread of "fitting" (weighted RMS error < 1) models at lower depths. We will push the models for FR1 and FR6 to be sure that they cannot have the same velocity at depth, but the results appear robust. There must be a strong difference between the sediments at FR1 and FR6: this kind of difference is hard to explain by lithology and we suspect that it is due to porosity and consolidation.

Interpretation

Sediment velocities/moduli

Shear moduli/velocities in consolidated marine sediments can be related to grain size and porosity using the Biot-Stoll [*Stoll*, 1977] model. These models, in which the sediment grains are cemented into a rigid framework that is infilled with fluids, predict a shear velocity of at least 1/2 the compressional velocity. That is, the shear velocities must be at least 0.8 km/s. The upper km at both sites is mostly below 0.8 km/s, indicating that the sediments are unconsolidated. There is no universally agreed-upon model for elastic wave propagation in unconsolidated sediments, with shear waves being a particular problem. Buckingham [1997; 1998; 2000] has recently proposed a model explaining unconsolidated sediment velocities. The basis of his model is that there is no skeletal framework and that the shear waves come as a result of grain-to-grain diffusion. Hamilton [1976] also compiled data on sediment shear velocities versus depth for various extracted samples, giving an empirical relation between shear velocity, grain size and porosity.

We are most interested in the Buckingham model and how it can explain the 5x difference in shallow shear velocities between sites FR1 and FR6. The model is based on the calculation of the "effective rigidity (shear) modulus", μ_s, which equals $\left(\frac{u_g}{u_0}\right)^{2/3} \mu_1$ at the sea surface and increases by $D^{2/3}$ with depth, where D is the subsurface depth, $\mu_1 = 5.1x10^7$ Pa is a constant of proportionality that coincides with the effective rigidity modulus or surficial sands, u_g is the mean grain diameter, u_0 is the reference grain diameter of 1000 μm (coarse sands). According to this theory, the 3-4 times lower shear velocities at FR6 than FR1 correspond to 30-60 times smaller grains at FR6. We can also calculate the mean grain size using the Buckingham formula, although the result should be taken with a grain of salt because the Buckingham model makes a few assumptions in its constant of proportionality, in its assumption of velocity increase with depth, and the modelisation they use hasn't been heavily ground-truthed. To

calculate the grain size, we must use a shear velocity/modulus that is within the zone where compliance is sensitive to changes with depth. We choose 0.4 km because it is at the shallow end of the well-constrained zone. There, $\mu = 0.035$+-0.01 GPa at FR6 and 0.35+0.05 GPa at FR1, indicating a mean grain size of 1.4 µm (clay) at FR6 and of 45µm (coarse silts) at FR1.

In **Figure 7**, we plot the compliance sites on reflection sections from seismic studies. There is no clear change in sediment units between the two sites, although we do not have a complete line connecting the 2. Site FR6 does seem to overly a thin layer of sediments (approximately 0.3 s thick in two way travel time, corresponding to 200-300 m thickness). This topmost layer appears to be a weaker seismic reflector than the seafloor elsewhere, so perhaps this is part of the low shear velocity material beneath this site? Our data also indicates that deeper velocities are lower at FR6, but very low velocities in the uppermost sediments could slightly exaggerate the difference.

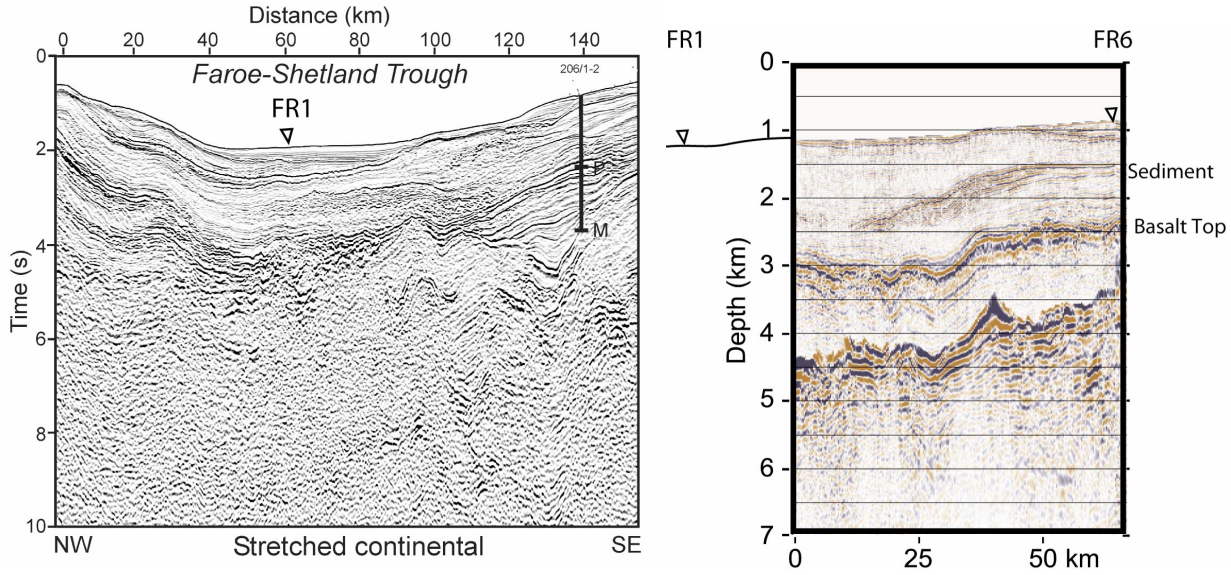

Figure 7: Position of compliance sites on reflection seismic profiles. Left: site FR1 on the ISIMM line. Right: sites FR6 and FR1 along the track of FLARE line 7 (FLARE line 7 does not extend to site FR1).

Infragravity waves

Why is there so much less infragravity wave energy at site FR6 than at FR1 and FR4? We had previously considered that infragravity wave energy would stay the same or increase as the water shallows because of bathymetric steering of the infragravity waves, but site FR6 is 20% shallower than FR1 or FR4.

One possibility is that the infragravity wave energy was everywhere lower during the FR6 deployment (that is, there is a strong temporal variation in infragravity waves). The three sites were deployed at different times: FR1 from 25 Nov 1720Z to 27 Nov 1140Z, FR4 from 27 Nov 1920Z to 29 Nov 1700Z and FR6 from 29 November 2323Z to 1 December 1520Z. We do not have a time series of infragravity wave energy at one site throughout the experiment, so we looked at the significant surface wave height in the region (**Figure 8**), calculated using the Wave Watch II model [*Tolman*, 1991; 1992; 1999]. Infragravity waves are thought to be generated by storms at or near coastlines that are "visible" (within the direct path of an ocean surface wave) from the measurement site. Note that the wave height over the measurement site is less important than that at the coastlines within its line of sight. There is no evidence that the infragravity wave energy was particularly low during the last deployment: in fact, deployment FR4 would appear to have the calmest infragravity wave conditions, as the coastal waters appear

particularly calm.

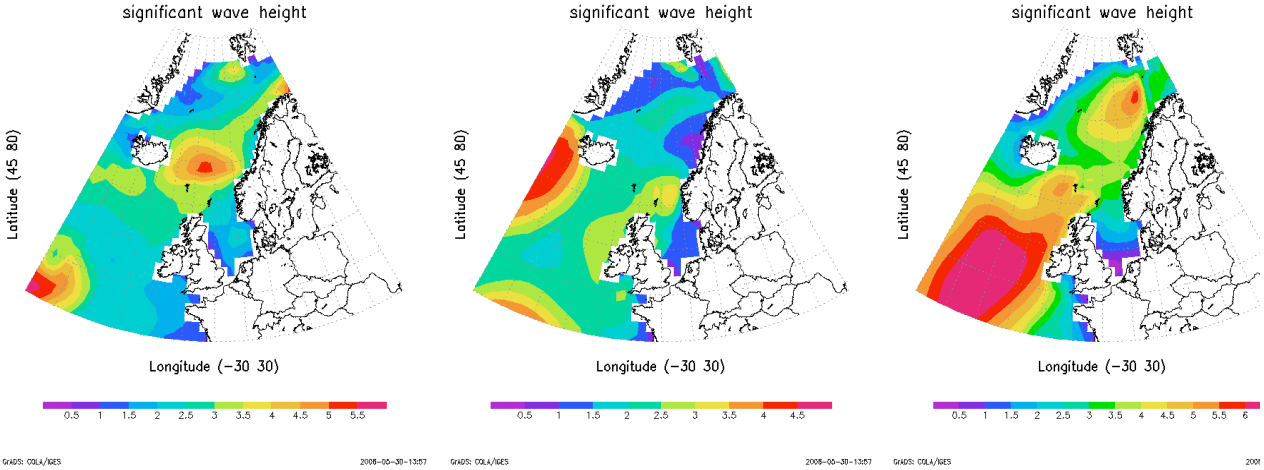

Figure 8: Significant wave heights at the middle of each compliance measurement. Left: 12h 26 November (site FR1). Middle: 12h 28 November (site FR4). Right: 00h 1 December (site FR6)

We conclude that the low infragravity wave energy at site FR6 is a bathymetric effect. We believe that most of the energy coming from higher latitudes that is steered towards the Faeroes islands was already steered there at higher latitudes, leaving energy to the south only in the middle of the basin where the waves go "straight".

Discussion and perspectives

Although the experiment did not see beneath the sub-basalt sediments, we were very pleased to note that the infragravity wave energy was largely sufficient to see beneath the basalts. Our main problem was the instrument tilting under seafloor currents. This could be eliminated either buy burying the seismometer or by developing a low-lying, tilt-resistant instrument package (currently a 17" glass ball on a 15" circular anchor). Performing compliance measurements during a period of weak tides would also reduce the tilt signal. Also, by reducing the gain of the horizontal channels we should be able to improve a larger subset of the vertical channel data. Finally, a fully non-linear correction for tilt may be necessary in these waters (we currently use a linearized correction, which is adequate as long as the instrument's off level is larger than the dynamic tilt under current forcing.

The inversions reveal a very large velocity difference in the sediments beneath the two sites, particularly near the surface. Site FR6, located near the southwestern bound of the basin, has much lower shear velocities, consistent with unconsolidated clays over at least the top 0.5 km. The shallow (upper 0.5 km) sediments at site FR1, in the middle of the basin and further to the north, are also unconsolidated but the 10x higher shear modulus indicates a much larger grain size, probably coarse silts to sands. Of course, the detailed structure could be much more complicated, with many different interlayered sediment types at either site, but the average trend is towards 30-60 times smaller sediment grains at FR6. With only two measurement sites, we cannot tell if this is a basin-wide trend or local pooling. In any case, we not recommend building a structure such as an oil platform or trying to drill through the sediments at site FR6!

That the very different sediment properties at the two sites could be due to local variations is underlined by the seismic static problem encountered by dense ocean-bottom cable reflection surveys. Shear wave

reflections are very difficult to align because of apparent rapid lateral changes in sediment shear velocities. Seafloor compliance measurements could help to quantify these changes, although many measurements would be needed.

Conclusions

Our seafloor compliance measurements were not sensitive to sub-basalt sediments, because of high tilt noise due to strong seafloor currents. The Faeroes basin is known for strong currents, and they can probably only be avoided by burying the seismometer. Short of burying the seismometer, the noise could be reduced by using a more stable, low profile seismometer package, reducing gain on the seismometer horizontal channels, and deploying during neap tides.

The infragravity wave signal ($10^{4.5}$ Pa^2/Hz at 2 of the 3 sites) is sufficient to detect sub-basalt sediments and constrain their shear modulus. The much lower signal at a site in the southwest end of the basin is probably due to bathymetric steering from sources that are principally to the north of the Faeroe Islands, not to temporal variations in these waves.

Shear moduli/velocities from about 0.3-0.5 km depth are about 0.035 GPa/0.1 km/s at site FR6 on the southwest edge of the basin (west of the basin axis) and 0.35 GPa/0.4 km/s at site FR1, in the middle of the basin farther to the north. These values indicate that the sediments are unconsolidated and suggest that the grain size is much smaller at site FR6. Calculations using the Buckingham (1998) model indicate primarily clays at FR6 and coarse silts at FR1.

Acknowledgments

We thank the SINDRI consortium for funding this research, and Trine Dahl-Jensen for her patience and help. We thank Jean-Xavier Dessa, Laurent Beguery, Oualid Aouji, Mark Roberts, Spahr Webb and Patrick Jonke for scientific, technical and logistic help

References

Bendat, J.S., and A.G. Piersol, Random Data: Analysis and Measurement Procedures, 566 pp., John Wiley and Sons, New York, 1986.

Bonnin, J., W. van Raaphorst, G.-J. Brummer, H. van Haren, and H. Malschaert, Intense mid-slope resuspension of particulate matter in the Faeroe–Shetland Channel: short-term deployment of near-bottom sediment traps, Deep-Sea Research 1, 49 (8), 1485-1505, 2002.

Buckingham, M.J., Theory of acoustic attenuation, dispersion, and pulse propagation in unconsolidated granular materials including marine sediments, J. Acoust. Soc. Am., 102 (5), 2579-2596, 1997.

Buckingham, M.J., Theory of compressional and shear waves in fluidlike marine sediments, J. Acoust. Soc. Am., 103 (1), 288-299, 1998.

Buckingham, M.J., Wave propagation, stress relaxation, and grain-to-grain shearing in saturated, unconsolidated marine sediments, J. Acoust. Soc. Am., 108 (6), 2796-2815, 2000.

Crawford, W.C., The sensitivity of seafloor compliance measurements to sub-basalt sediments, Geophys. J. Int., 157, 1130-1145, 2004.

Crawford, W.C., and S.C. Webb, Removing tilt noise from low frequency (<0.1 Hz) seafloor vertical seismic data, Bull. Seis. Soc. Am., 90 (4), 952-963, 2000.

Crawford, W.C., S.C. Webb, and J.A. Hildebrand, Seafloor compliance observed by long-period pressure and displacement measurements, J. Geophys. Res., 96 (10), 16151-16160, 1991.

Crawford, W.C., S.C. Webb, and J.A. Hildebrand, Estimating shear velocities in the oceanic crust from compliance measurements by two-dimensional finite difference modeling, J. Geophys. Res., 103 (5), 9895-9916, 1998.

Fliedner, M.M., and R.S. White, Depth imaging of basalt flows in the Faeroe-Shetland Basin, Geophys. J. Int., 152, 353-371, 2003.

Fruehn, J., M. Fliedner, and R.S. White, Integrated wide-angle and near-vertical subbasalt study using large-aperature seismic data from the Faeroe-Shetland region, Geophysics, 66 (5), 1340-1348, 2001.

Gallagher, B., Generation of surf beat by non-linear wave interactions, J. Fluid Mech., 49 (1), 1-20, 1971.

Guza, R.T., and A.J. Bowen, Finite amplitude edge waves, J. Mar. Res., 269-293, 1976.

Hamilton, E.L., Shear-wave velocity versus depth in marine sediments: a review, Geophysics, 41 (5), 985-996, 1976.

Herbers, T.H.C., S. Elgar, and R.T. Guza, Infragravity-frequency (0.005-0.05 Hz) motions on the shelf. Part I: Forced waves, Journal of Physical Oceanography, 24, 917-927, 1994.

Herbers, T.H.C., S. Elgar, and R.T. Guza, Generation and propagation of infragravity waves., J. Geophys. Res., 100 (C12), 24863-24872, 1995a.

Herbers, T.H.C., S. Elgar, R.T. Guza, and W.C. O'Reilly, Infragravity-frequency (0.005-0.05 Hz) motions on the shelf. Part II: Free waves, Journal of Physical Oceanography, 25, 1063-1079, 1995b.

Hughes, S., P.J. Barton, and D. Harrison, Exploration in the Shetland-Faeroe Basin using densely spaced arrays of ocean-bottom seismometers, Geophysics, 63 (2), 490-501, 1998.

Hughes, S., P.J. Barton, and D.J. Harrison, Characterizing the Mid-Faeroe Ridge using seismic velocity measurements, J. Geophys. Res., 102 (4), 7837-7847, 1997.

Jones, G., Sub-basalt imaging using long offset data in the tau-p domain, Lithos Science Report, 5, 49-59, 2003.

Latychev, K., and R.N. Edwards, On the compliance method and the assessment of three dimensional sea floor gas hydrate deposits, Geophys. J. Int., 155 (3), 923-952, 2003.

Martini, F., and C.J. Bean, Application of pre-stack wave equation datuming to remove interface scattering in sub-basalt imaging, EAGE 63rd Conferenc & Technical Exhibition,, O-17, 2001.

Masson, D.G., R.B. Wynn, and B.J. Bett, Sedimentary environment of the Faroe-Shetland and Faroe Bank Channels, north-east Atlantic, and the use of bedforms as indicators of bottom current velocity in the deep ocean, Sedimentology, 51, 1207-1241, 2004.

Okihiro, M., R.T. Guza, and R.J. Seymour, Bound infragravity waves, J. Geophys. Res., 97 (C7), 11453-11469, 1992.

Richardson, K.R., J.R. Smallwood, R.S. White, D.B. Snyder, and P.K.H. Maguire, Crustal structure beneath the Faroe Islands and the Faroe-Iceland Ridge, Tectonophys., 300, 159-180, 1998.

Snodgrass, F.E., G.W. Groves, K.F. Hasselmann, G.R. Miller, W.H. Munk, and W.H. Powers, Propagation of ocean swell across the Pacific, Phil. Trans. Roy. Soc. A, 259, 432-497, 1966.

Stoll, R.D., Acoustic waves in ocean sediments, Geophysics, 42 (4), 715-725, 1977.

Tolman, H.L., A third-generation model for wind waves on slowly varying, unsteady and inhomogeneous depths and currents, J. Phys. Oceanogr., 21, 782-797, 1991.

Tolman, H.L., Effects of numerics on the physics in a third-generation wind-wave model, J. Phys. Oceanogr., 22, 1095-1111, 1992.

Tolman, H.L., User manual and system documentation of WAVEWATCH-III version 1.18, in NOAA/NWS/NCEP/OMB Technical Note, pp. 110, 1999.

Webb, S.C., Broadband seismology and noise under the ocean, Rev. Geophys., 36 (1), 105-142, 1998.

Webb, S.C., X. Zhang, and W.C. Crawford, Infragravity waves in the deep ocean, Journ. Geophys. Res., 96 (C2), 2723-2736, 1991.

White, R.S., P.A.F. Christie, N.J. Kusznir, A. Roberts, A. Davies, N. Hurst, Z. Lunnon, C.J. Parkin, A.W. Roberts, L.K. Smith, R. Spitzer, A. Surendra, and V. Tymms, iSIMM pushes frontiers of marine seismic acquisition, First Break, 20, 782-786, 2002.

White, R.S., J. Fruehn, K.R. Richardson, E. Culen, W. Kirk, J.R. Smallwood, and C. Latkiewicz, Faeroes large aperture research experiment (FLARE): imaging through basalt, in Petroleum Geology of Northwest Europe: Proceedings of the 5th Conference, edited by A.J. Fleet, and S.A.R. Boldy, pp. 1243-1252, Geological Society, London, 1999.

White, R.S., and D. McKenzie, Magmatism at rift zones: the gerneration of volcanic continental margins and flood basalts, J. Geophys. Res., 94 (6), 7685-7729, 1989.

White, R.S., J.R. Smallwood, M.M. Fliedner, B. Boslaugh, J. Maresh, and J. Fruehn, Imaging and regional distribution of basalt flows in the Faeroe-Shetland Basin, Geophysical Prospecting, 51, 215-231, 2003.

Yamamoto, T., and T. Torii, Seabed shear modulus profile inversion using surface gravity (water) wave-induced bottom motion, Geophys. J. R. Astr. Soc., 85, 413-431, 1986.

Yamamoto, T., M.V. Trevorrow, M. Badiey, and A. Turgut, Determination of the seabed porosity and shear modulus profiles using a gravity wave inversion, Geophys. J. Intl., 98 (1), 173-182, 1989.

Ziolkowski, A., P. Hanssen, R. Gatliff, X.-Y. Li, H. Jakubowicz, and G. Hampson, Low frequency sub-basalt imaging, in EAGE 64th Conference & Exhibition, pp. Z-99, Florence, Italy, 2002.